Available online at www.scientiaresearchlibrary.com

Scientia Research Library

ISSN 2348-0408
USA CODEN: JACOGN

Journal of Applied Chemistry, 2014, 2 (1):109-127
(*http://www.scientiaresearchlibrary.com/arhcive.php*)

Flow Analysis in the Core of Pebble Bed High Temperature Gas-Cooled Reactor

AndréAugusto Campagnole dos Santos, Amir Zacarias Mesquita[1], Franklin Candido Costa,Sincler Peixoto de Meireles, and Hugo Cesar Rezende
Nuclear Technology Development Center, Brazilian Nuclear Energy Commission (CDTN/CNEN), Belo Horizonte (MG), Brazil

---

ABSTARCT

This paper presents a numerical investigation of thermal-fluid dynamics processes through the gaps of the spherical fuel elements (fuel pebbles) in the core of a Pebble Bed Reactor (PBR), using Computational Fluid Dynamics (CFD). The PBR is a Very High Temperature Reactor (VHTR) design to the Generation IV International Forum (GIF). The PBR is one of the most promising projects of the seven(originally six) classes of GIF reactors. The set of pebbles that constitute the core was modeled by representations of crystalline structure with different packing factors. The results shown the importance of simulation of heat conduction inside the pebble fuel as well as the need to better assess the influence of the arrangement formed by pebbles fuel in PBR reactors thermal-fluid dynamics behavior.

Keywords: Very High Temperature Reactor (VHTR); Computational Fluid Dynamics (CFD); PBR reactors

---

INTRODUCTION

A Very High Temperature Gas-cooled Reactor (VHTR) is one of the renewed reactor designs to play a role in nuclear power generation. The Generation IV International Forum findings relative to the future nuclear systems (sustainability, security and reliability, economy, non-proliferation and physical protection) have given new impetus to graphite-moderated VHTRs. These reactors design concept is currently under consideration and development worldwide. The high modular VHTR concept exhibits inherent safety features due to the low power density and the large amount of graphite present in the core, which gives a large thermal inertia in the event of accidents as loss of coolant. These passive concepts were first introduced in German HTR-Module (pebble fuel) design (Lohnert, 1990) (Lohnert, and Reutler, 1983). The fuel design of fissile kernels coated with carbon and silicon carbide layers mixed with graphite is suitable for reaching very high burn up and ensures a full confinement of volatile fission products during normal and abnormal situations. The combination of coated particle fuel, inert helium gas as coolant and graphite moderated reactor

makes possible to operate at high temperature yielding a high efficiency. Other characteristics of VHTR are the capability of providing high temperature heat and suitability for various power conversion cycles (Hassan, 2008). They will be capable of delivering high temperature helium (up to 950 °C) either for industrial heat application or directly to drive gas turbines for electricity (the Brayton cycle) with about 48% thermal efficiency possible. Technology developed in the last decade makes HTRs more practical than in the past, though the direct cycle will be a further technological step, which means that there must be high integrity of fuel and reactor components (Lacy, 2011).

There are two core concepts of VHTR, the prismatic block-type and the pebble bed-type. The first type follows the line of the High Temperature Engineering Test Reactor (HTTR) developed and built by Japan initially with coolant exit temperature of 850 ^{o}C and then 950 ^{o}C in April 2004. The second is the result of the German program, which was later imported by China and developed in the Republic of South Africa as the Pebble Bed Modular Reactor (PBMR) (Duarte at. al, 2013).

This paper presents a numerical investigation of flow and heat transfer between the coolant and fuel spheres present in the core of a PBR using the CFD code CFX 14.0 (Ansys, 2012). This study is an initial step in the development of procedures for the numerical simulation of transport phenomena and advanced reactors safety analysis under Brazilian Institute of Science and Technology (INCT).

MATERIALS AND METHODS

In pebble-bed reactors the fuel is contained in pebbles of graphite rather than in metallic rods which are used in reactors like the BWR (Boiling-Water Reactor) and PWR (Pressurized Water Reactor). The graphite pebbles of typically 60 [mm] in diameter contain about 5000 to 20.000 coated TRISO (*Tristructural-Isotropic*) particles. These TRISO particles contain a fuel kernel of UO_2. The pebble-bed reactor has two major benefits. The first one is because of the gas coolant, since the pebbles can moderate themselves (they are like minireactors) the reactor can be cooled with an inert gas like helium. An inert gas is not reactive under normal circumstances and the gas does not get radioactive as fast as water, which is used in conventional PWR. Because of the higher working temperature of the reactor the energy conversion efficiency improves. The low power density and high temperature resistance of the core materials ensure that any decay heat will be dissipated and transported to the environment without the decay heat causing a meltdown (Dijk, 2008).

In the core of the pebble-bed reactor there might be two types of balls, namely graphite and fuel balls. The graphite balls fill the cylindrical center of the pebble-bed and fuel balls surround the graphite balls. Both the graphite and the fuel balls are extracted from the bottom and reinserted (or replaced in case of burn up) on the top of the pebble-bed. This extracting and reinserting gives rise to a ball velocity of about 4.5[mm/h] [4]. Since this flow is slow we can approximate the pebble-bed as a fixed packed bed (Dijk, 2008). A model of the core of a PBR is shown in Fig. 1 (Lee et al, 2007).

In Germany a pebble-bed reactor, the AVR (working group test reactor) was build in the sixties to serve as a showcase experimental reactor and as a showcase to how safe this new form of technology was. However in the year 1988, after 21 years of service, the reactor was shutdown. Currently there is one working prototype of the pebble-bed reactor in China the so called HTR-10, standing for High Temperature Reactor (10MW). Multiple pebble-bed reactors are being designed for construction in South Africa to supply a large part of their energy needs and accepting pebble-bed reactors as a solution to their growing energy consumption (Dijk, 2008).

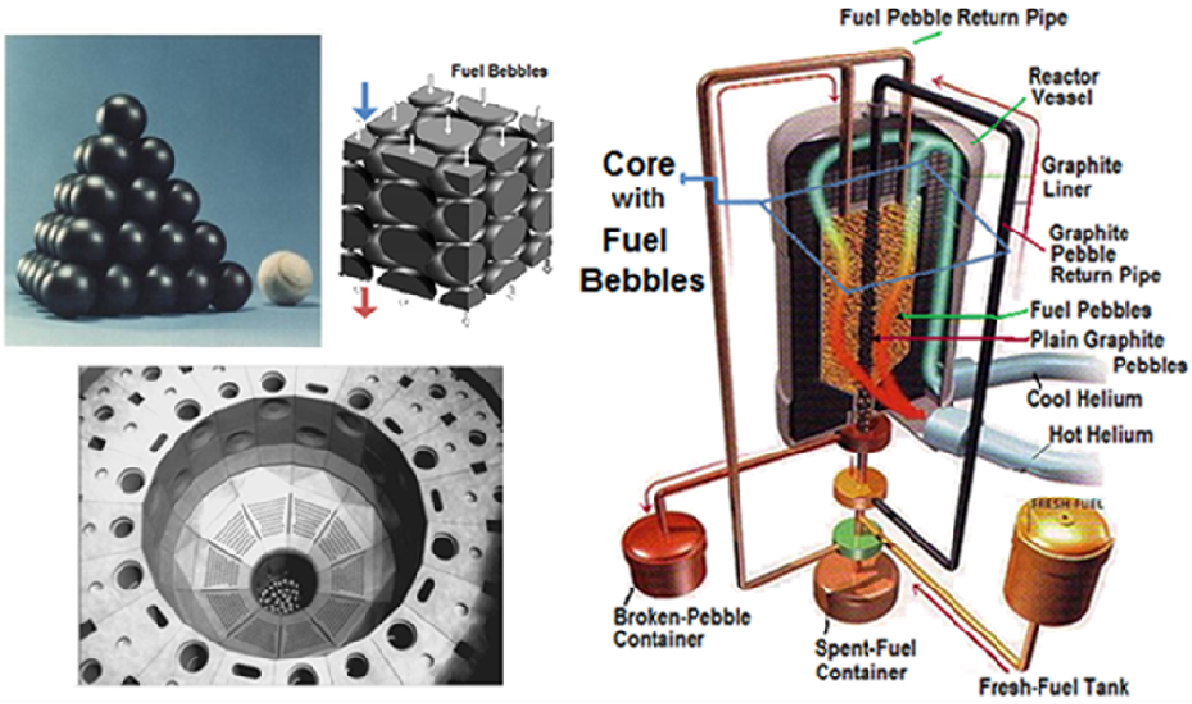

Figure 1.Diagram of thePebble Bed Reactor (PBR) (Lee et al, 2007).

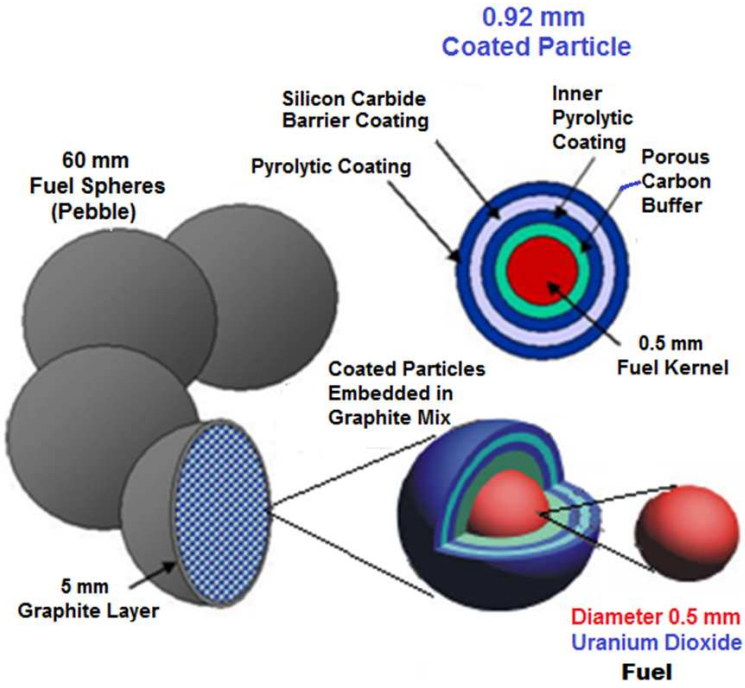

Figure 2.The TRISO sphere and the pebble fuel (Duarte et al., 2013).

This type of reactor is claimed to be passively safe (negative coefficient of reactivity) that is, it

removes the need for redundant, active safety systems. Because the reactor is designed to handle high temperatures, it can cool by natural circulation and still survive in transient scenarios, which may raise the temperature of the reactor to 1600 °C. Because of its design, its high temperatures allow higher thermal efficiencies than possible in traditional nuclear power plants (up to 50%) and have the additional feature that the gases do not dissolve contaminants or absorb neutrons as water does, so the core has less in the way of radioactive fluids (Hassan, 2008).

Because of the multi layers, the pellets are extremely heat resistant, able to reach temperatures around 1600°C. In addition, due to the high durability of the pellets, it is difficult to remove the trapped fission products and ultimately discourages proliferation. Waste disposal also becomes easier as the fuel is concentrated.

In pebble bed reactor cores, the gas flows around randomly distributed spheres. The understanding of such complex unsteady flows is important. This requires a variety of analysis techniques and simulation tools. These range from simple one-dimensional models that do not capture all the significant physical phenomena to large scale three dimensional computational fluid dynamics (CFD) codes (Hassan, 2008) (Lee et al., 2007a, b) (Sobes et al., 2011).

In these studies, the random arrangement of pebbles fuel inside the reactor vessel has simplified by representations of the crystalline structures. These structures are characterized by a packing factor, defined as the fraction of volume occupied by the solid spheres. Other considerations in the numerical simulations of the pebble bed reactors are the spacing between the balls and prescription of a heat flow on the surface of spherical fuel. These considerations reduce the number of mesh nodes, but not realistically reproduce the flow in this reactor.

Lee et al. (2007b) simplified the spheres arrangement by crystalline structures of face-centered cubic (CFC), and body-centered cubic (CCC) given spacing between adjacent spheres of 1 mm and the estimated flow on its surface. Lee et al. (2007a) studied the simplification of the spacing between the fuel pebbles in the simulations. Hasan (2007) studied the simulation of turbulent transport for the gas through the gaps of the spherical fuel elements using the large eddy simulation. He investigated a structure composed of 24 spheres in point contact and flux prescribed on their surfaces. Sobes et al. (2011) suggested the investigation of flow structures with high packing factor, as the structures FCC and HC (hexagonal compact).

Two analyzes were performed recentlyby Santos et al. (2013). In this present paper, the results of a third analysis will be presented.In the first analysis were evaluated two models the heat transfer to the fuel spheres. Being a model with volumetric heat generation with thermal conduction, in the fuel and in the cladding. In another model was estimated heat flux at the surface of the spheres, simplifying the simulation. For each of these models were studied two cases, one considering spacing of 2 mm between the balls (no contact - SC) and another considering contact between them (contact - CC). The aim of this study was to evaluate the differences between these two mechanisms of heat generation.

In the second analysis it was evaluated the influence of the arrangement of spheres in thermal and fluid dynamic behavior of the pebble bed (Santos et al. 2013). The assembly that constitutes the pebble bed was modeled representing the crystal structures. As the arrangement of spheres is variable in PBR core reactors, it was studied models with different packing factors (Auwerda et al., 2010).

Geometries and Boundary Conditions

Fuels and boundary parameters used in the analyzes are at a Pebble Bed Modular Reactor - PBMR with a power of 400 MW(t) shown in Table 1 (Matzner, 2004).

Table 1.*Operational parameters of the PBMR - 400 MW reactor*

Parameter	Values
Core Reactor Power	400 MW(t)
Coolant	Helium
Fluid Flow	185 kg/s
System Pressure	9 MPa
Inlet/Outlet Temperatures	500 / 900 ^{o}C
Number of fuel Spheres in the Core	451 000
Tank Diameter/Internal Reflector	3.7 / 2.0 m

The geometries simulated in the first phase of this study are composed of two spheres contained in a volume in the shape of a rectangular prism as shown in Figure 3. The spheres are aligned in the y direction, and 60 mm from the top and equidistant from the vertical center line of the prism (x = 90 mm, y = 120 mm, z = z mm). The side faces of the prism walls were considered symmetrical. The top was defined as fluid inlet with uniform velocity of 5 m/s and a temperature of 900 °C, conditions on the bottom of the reference reactor core. The bottom was defined as output with zero relative pressure.

Four variations were simulated by varying the geometry of this distance between the centers of the spheres and the model of heat generation. Table 2 presents the data from the four simulated cases. In the case of volumetric heat generation in the fuel, three domains were created: one for the fluid, one for fuel and one for the cladding. In the case of estimated heat flux at the surface of the spheres was created just the domain of the fluid. The step between spheres is smaller than the diameter of the spheres in models with contact (CC Flow and CC Volumetric), which generates a circular contact area of a diameter of 2.4 mm. This contact area was estimated based on the deformation of the spheres caused by the gravitational load present in the lower region of the reactor (Lee et al. 2007a). In the regions of contact between spheres was not considered the heat transfer resistance. The surfaces of the spheres were considered smooth and without imperfections.

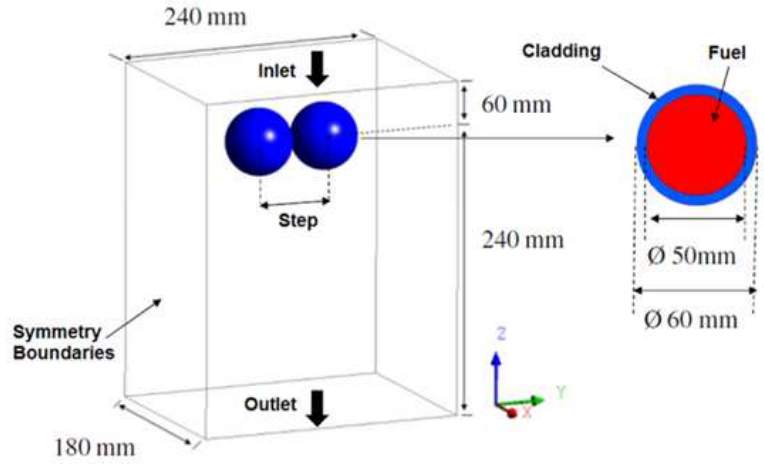

Figure 3.Geometry simulated in the analysis

Table 2. Simulations

Cases	Flow SC	Flow CC	Volumetric SC	Volumetric CC
Step Between Spheres (mm) Heat Generation Model	62 Prescribed the flow on surface	59.952	62 Volumetric heat generation	59.952

It was adopted the values of 14.75 MW/m³ for the rate of volumetric heat generation in the fuel and 85.36 kW/m^2 for the heat flux at the pebbles surface, based on data of Lee et al. (2007a).

Based on the results of the first analysis step was defined between the spheres. It was also defined the generation model suitable for simulation performed arrangements of spheres in the second analysis. Modeled in this study were based on the arrangements of spheres crystal structures: simple cubic (CS), the body centered cubic (CCC) and face-centered cubic (CFC), shown in Figure 4. The dimensions of the simulated cubes were calculated to be representative of the arrangement of spheres maintaining a sphere centered in the domain. Table 3 shows the characteristics of the simulated arrays.

The surface arrangements with higher Z were defined with inlet uniform temperature of 900 °C. The input flow in each model ($\dot{m}_{model}$) was estimated according to Equation 1 considering the flow in the reactor ($\dot{m}_{PMBR}$), the cross-sectional area of the reactor core (A_{PBMR}), and cross-sectional area of the model (A_{model}).

$$\dot{m}_{modelo}=\dot{m}_{PBMR}\left(\frac{A_{modelo}}{A_{PBMR}}\right) \quad (1)$$

The cross-sectional area of the reactor core was calculated using Equation 2 with the values of the diameter of the tank (D_T) and the diameter of the reflector center (D_C).

$$A_{PBMR}=\frac{\pi}{4}(D_T^2-D_C^2)=7.61\ \text{m}^2 \quad (2)$$

The flow in the reactor core has been obtained from the data of Table 1. The cross-sectional area of each model is A_{CS}= 0.01438 m², A_{CCC} = 0.01917 m², A_{CFC} = 0.02875 m². Therefore, the flow in each model is $\dot{m}_{CS}$ = 0.3495 kg/s, $\dot{m}_{CCC}$ = 0.466 kg/s, $\dot{m}_{CFC}$ = 0.699 kg/s.

The frontier output with lower Z face was set with zero relative pressure, where output and fluid inlet were permitted. The boundaries of adjacent field of fluid interfaces have been defined as translational periodicity to allow entry and exit of fluid. The faces of the fuel cladding and the edges of the field were considered as interfaces of symmetry. The geometries created are shown in Figure 4 and their characteristics are presented in Table 3.

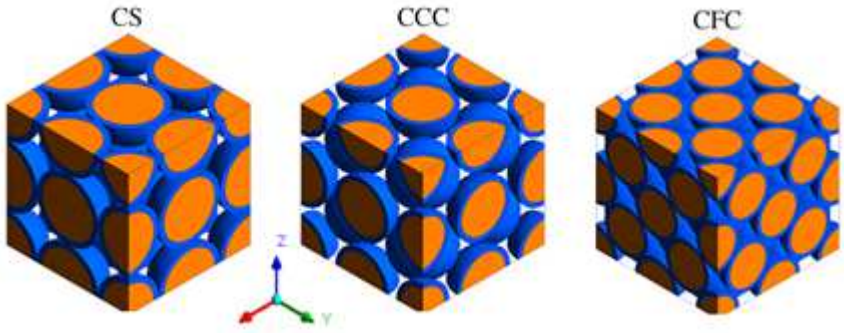

Figure 4.Geometries simulated in the analyzes

Table 3. Characteristics of simulated arrangements

Parameter	CS	CCC	CFC
Packing Factor	0.52	0.68	0.74
Cube Length (mm)	120	138	170
Total Number of Simulated Spheres	8	16	32
Number of Spheres in Contact with the Central Sphere	6	8	12

Materials Properties

The thermodynamic properties of the fuel were found in Lee et al. (2007a) and evaluated using Equations 3 and 4, where K_{fuel} is the fuel thermal conductivity fuel (J/mK) and $c_p$the fuel specific heat (J/kgK).

$$K_{fuel} = 127.68\left(\frac{0.06829-0.3906x10^{-4}T}{10^{21}+1.931x10^{-4}T} + 1.228x10^{-4}T + 0.042\right) \quad (3)$$

$$c_{p_{fuel}} = \frac{1.75x10^{6}}{1781.78}(0.645 + 3.14x10^{-3}T - 2.809x10^{-6}T^{2} + 0.959x10^{-9}T^{3}) \quad (4)$$

The thermodynamic properties of graphite were obtained from Tak et al. (2008). The properties of helium were obtained from the NIST (2013) database. Figure 5 shows the modeling of the contact between spheres .

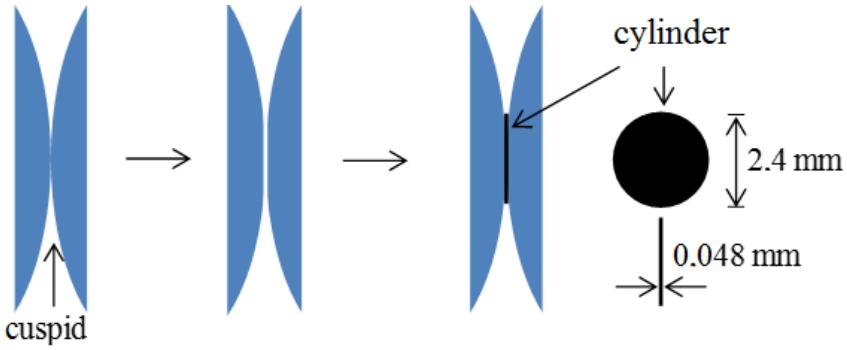

Figure 5. Modeling of the contact between spheres

Mesh

Were generated unstructured tetrahedral mesh for all cases of two analyzes. In all layers of mesh are generated prismatic elements, called *Inflation* to the surfaces of the pebbles in the domain of the fluid, and for cases with volumetric heat generation in the fluid-coating interface and coating-graphite in the field of fuel and fuel. There were five layers of specified *Inflation* with smooth transition between the last layer of tetrahedral mesh and the first prism and the growth rate of the layers of high *Inflation* equal to 1.2. In cases of contact between the spheres used was a refinement

edge contacts with pebbles fuel element size equal to 0.1 mm. Next the surfaces of the spheres the size of elements was set to 2 mm with an expansion allowable size of 1.2 to 5 mm. Node number of cases with volumetric heat generation and prescribed on the surface of the pebbles of the first analysis were equal to ~ 350,000 and ~ 230,000, respectively.

Based on the results of the first analysis were generated meshes of the arrangements CS, CCC and CFC, considering contact between the balls and volumetric heat generation in each (Santos et al. 2013). Meshes generated in arrangements showed a high number of nodes in the region of contact between spheres, especially for the CFC arrangement that has the largest number of contacts per sphere. The number of nodes of arrangements CS, CCC and CFC were equal to 2,174,794, 5,924,297 and 14,829,636, respectively.

In the cylinder contact were generated prismatic elements by the method of extrusion with triangular elements in the extrusion face (face in contact with the ball). In the field of fluid were created prismatic elements known as inflation layers at the surface of fuel pellets . In other regions the mesh consisted of tetrahedral elements. The dimensional parameters of meshes are shown inTable 4.

Table 4 shows the total number of mesh nodes (fluid and solid domain) and the domain of the fluid divided by the number of balls of each model. The number of nodes per ball in the field is necessary to achieve independence of numerical results relative to the mesh used in simulations of flow in beds of pebbles fluid is approximately 190000 (Mclaughlin et al., 2008). According to Table 4 and this information, the number of nodes in the fluid is insufficient to ensure the independence of the result in relation to the mesh.

Table 4.Dimensional parameters and characteristics of the meshes.

	CS	CCC	CFC
Minimum element size [mm]	0.169	0.169	0.100
Maximum element size [mm]	4.255	4.255	2.500
Maximum element size in the fluid [mm]	2.028	2.028	1.200
Number of inflation layers	9	9	5
Total number of nodes	707988	1712741	5787406
Number of nodes in a fluid sphere	67731	59556	124764

Figure 6 shows the three meshes generated in a plane passing through the contacts. There is a high density of elements in the vicinity of the contact.

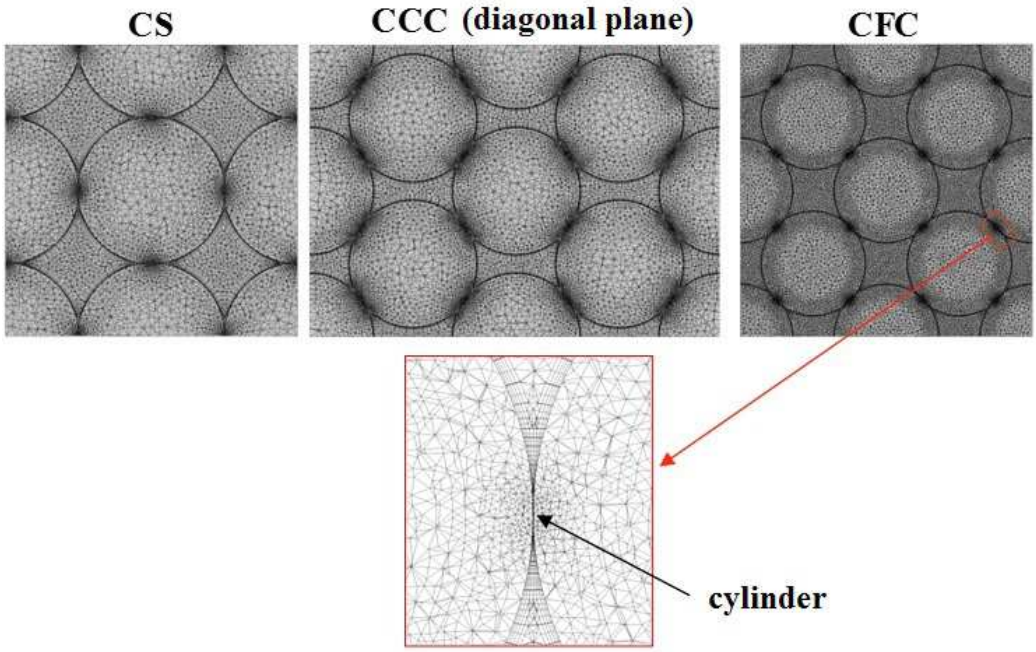

Figure 6.Meshes used and detail of the contact

Boundary conditions

The parameters of the PBMR - 400 MWdescribed in Table 1 were used as reference. In the first analysis, the lateral faces of the prism are considered symmetrical walls. The upper face is defined as a uniform fluid inlet speed of 5 m / s and temperature of 900 °C. Conditions from the bottom of the reactor core by reference. The lower face was set to output at zero relative pressure. The boundary conditions of the second and third analysis are described below.

At the inlet was defined with helium flowing normal to the surface temperature of 900 ° C to simulate the lower core region of a PBR reactor. The normal condition of overland flow at the entrance is unreal. A better alternative would be to define periodic boundaries between the input and output flow to prescribing a way to create a velocity profile at the entrance. This was not done because the Ansys CFX 14.0 does not allow this type of border in simulations in which it defines a fluid with variable properties (Ansys, 2012). The input flow in each model ($\dot{m}_{model}$)was estimated according to Equation 5 considering the flow in the reactor $\dot{m}_{PBMR}$, the cross-sectional area of the reactor core reactor (A_{PBMR} = 7.62 m^2 and cross-sectional area model A_{model}.

$$\dot{m}_{model} = \dot{m}_{PBMR}\left(\frac{A_{model}}{A_{PBMR}}\right) \quad (5)$$

Flow rates of CS , CCC and CFC models found by Eq. 5 were equal to 0.3495 kg/s, 0.466 kg/s and 0.699 kg/s , respectively. In the reactor it is expected that a distribution of flow throughout their cross section to occur due to variations in porosity in a radial direction of the core. For a larger mass flow will tend to be directed to the regions in which they occur less pressure loss of the flow.Therefore , a better estimate of flow in each structure would be obtained if it were considered that effect the distribution of mass flow . The relative pressure of the system was set equal to 9 MPa. On output was specified relative pressure of 0 Pa, this border was allowed entry and exit of

the fluid according to the pressure field. This condition is defined as opening by the software Ansys CFX 14.0 (Ansys, 2012). Picked up this type of boundary condition due to recirculation in this region . The turbulence intensity at the inlet and outlet was specified at 5 % . The other boundaries of the domain of the fluid were defined as periodic. The boundary condition was defined as fuels symmetry. In the fuel core matrix was prescribed a uniform heat generation volume equal to 14.75 MW/m³ (Lee et al. 2007a). This value was found by dividing the thermal reactor power by the volume of the core matrix of all spheres in the reactor. Figure 7 schematically shows the boundary conditions defined for the three models shown in CFC structure.

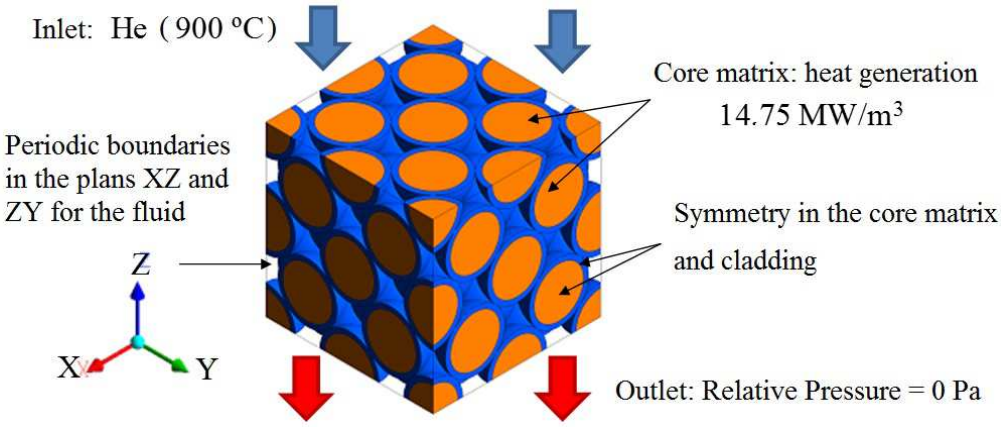

Figure7.Boundary conditions.

Numerical Parameters

The Reynolds-averaged Navier-Stokes equations (RANS) with the turbulence model k-ε and the energy equation were solved in the simulations using the code CFX 14.0 which is based on the method of finite volume (Ansys, 2012).The terms of all the equations have been discretized by high-resolution scheme, formally second order. In the simulations the transient temporal terms were discretized by Euler scheme of second order.

The calculations were performed in parallel for six Dell computers with two Intel Xeon 2.27 GHz processors and 24 GB of RAM memory each. The first analysis of the simulations was performed in steady-state. The virtual time step used was equal to 0.01 s for the fluid and 1 s to the solid (Costa et al. 2011).

In the second analysis the three arrangements were initially simulated in steady-state with virtual time step equal to 0.0001 s for the fluid and 1s to the solid. Simulations under permanent non-converged with 500 iterations, and it were decided to use the results of the 500th iterations as initial condition for transient simulations. The full transient simulation for cases CS and CCC was equal to 1s with a time step equal to 0.005 s, achieving convergence with waste RMS of ~ 10^{-5}. For the CFC arrangement, with greater difficulty convergence was simulated a total time equal to 0.1 s with a time step between 0.00025 s getting a RMS> 10^{-4}.

RESULTS AND DISCUSSIONS

Figure 8 shows the temperature distribution on the surface of the central area of each structure in time equals 0.1 s. The flow is downward (z-direction).

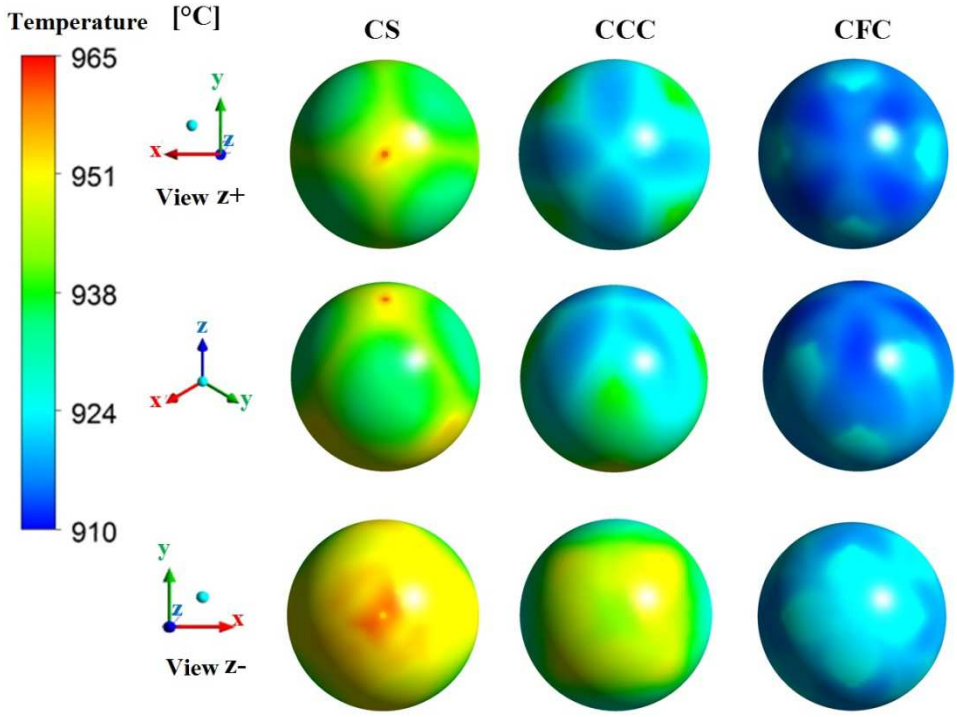

Figure 8.Temperature distribution on the surface of the central sphere structures.

Figure 9 showsthe distribution ofsurface temperatureof the centerof eachspheremodelin spherical coordinates. The angles, azimuth(θ) andpolar(φ) are definedin Figure 10, where φequals 0°correspondsto the upper regionof the sphereandφequal to 180°to the lowerregion.

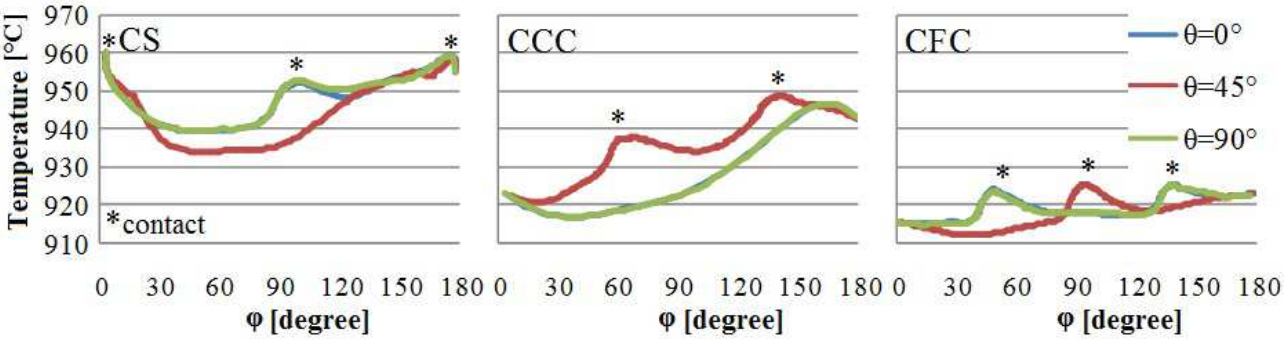

Figure 9.Temperature distribution on the surface of the central sphere.

Figures 8 and 9 show higher variations (about 30 °C) on the surface of the central sphere of CS CCC models. It can noted temperature peaks in the regions of contact between spheres, indicated by [*] in Figure 9. It is noted symmetry in temperature distribution lines with θ equal to 0 ° and 90 ° in each model. The maximum variation of surface temperature in relation to the temporal mean was 1 ° C.

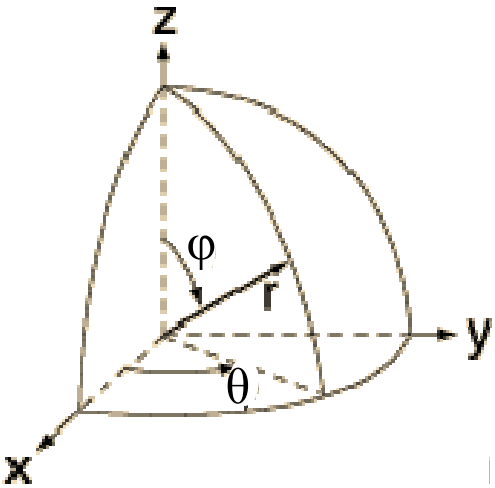

Figure 10.Definition of polar (φ) and azimuthal (θ) angles

Figure 11 shows the distribution of the Nusselt number (Nu) in the central sphere at the end of the simulations. The Nusselt number location varies considerably on the surface of the fuel. Note a greater ability to remove heat from the fluid fuel in CFC structure. It was also noticed a decrease in heat transfer in the lower region of contacts in all structures.

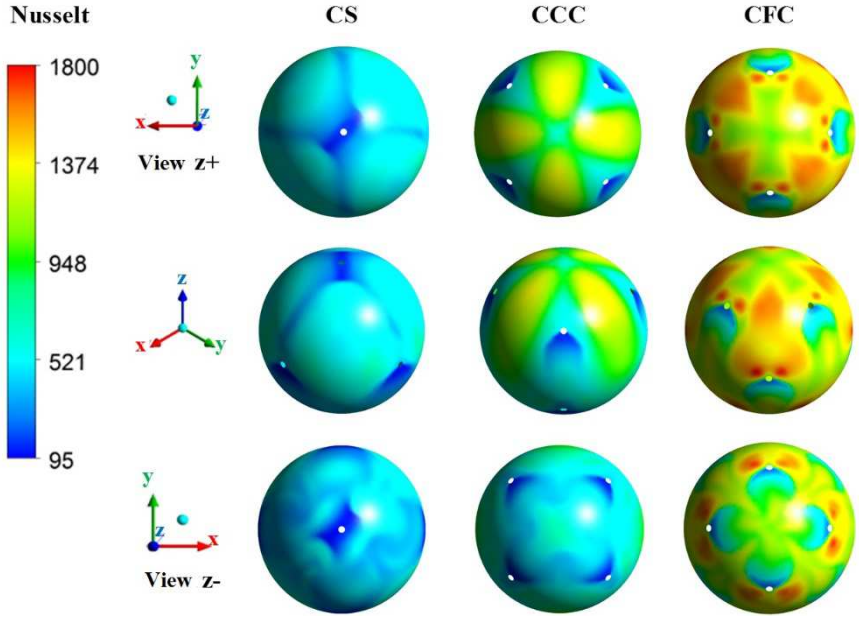

Figure 11.Distribution of the local Nusselt number in the central sphere

Achenbach (1995) proposed a correlation for the Nusselt number in a pebble bed as a function of *Reynolds* number (Re), the *Prandtl* number (Pr), and the packing factor (FE). Equation 6 describes the correlation combining the laminar *Nusselt* numbers (Nu_l) and turbulent (Nu_t), which are defined in Equations 6 and 7, respectively. Equation 8 is valid for FE between 0.065 and 0.74, Pr equal to 0.7 to 10^4 and value of *Re*/(1-FE) *Re* / (1-EF) equal to 7.7 x10^5.

$$Nu_l = 0{,}664 Pr^{1/3} \left(\frac{Re}{1-FE}\right)^{0{,}5} \quad (6)$$

$$Nu_t = \frac{0{,}037 (Re/(1-FE))^{0{,}8} Pr}{1+2{,}443 (Re/(1-FE))^{-0{,}1} \left(Pr^{2/3}-1\right)} \quad (7)$$

$$Nu = (1 + 1{,}5FE)\left(2 + \left(Nu_l{}^2 + Nu_t{}^2\right)^{0{,}5}\right) \quad (8)$$

Table 5 shows the *Nusselt* (*Nu*) number obtained by Eq. 8. The *Nu* mean in the sphere obtained numerically. The *Pr* and *Re* numbers estimates in the simulations were equal to 0.657 and 27370, respectively. This number *Pr* is not within the range of application of Eq. 8. However, as the value is close to the applicable and no other correlation was found, the Eq. 8 was used for results comparison.

Table 5.Nusselt Number.

	CS	CCC	CFC
Nu (correlation)	427	639,6	772
*Nu*average(numerical)	470,1	728.1	1202.7
Difference [%]	10.1	13.8	55.8
Range of*Nu* (numerical)	95-722	128-1392	232-1797

The average Nusselt number at the center of the sphere of structures CS and CCC differ from the correlation found in Achenbach (1995), at around 10%. Although the packing factor and Reynolds number of CFC simulation model are within the range of Eq. 8 applies to the difference between the number average *Nu* and *Nu* obtained from the correlation was equal to 56%. It is believed that the turbulence model *Standard k-ε* used in the simulations could not calculate the flow in a manner acceptable in CFC structure resulting from this difference. The Nu calculated by the correlation is within the range of *Nu* in the central sphere numerically obtained in all structures.

The flow lines around the central area of each model are shown in Fig. 12. Can be noted higher gas velocities in the CFC model, the order of 82 m/s, and lower gas velocities in the CS model, with a top speed around 45 m/s. Observed that the vortex shedding in the lower region of the contact points between the spheres. The streamlines of the flow vortices present in low speeds resulting in low heat transfer coefficients in the region of contacts as can be seen in Fig. 12.

Figure 13 shows the temperature distribution in the central sphere in a plane passing through the center of the end of simulations. It is observed from Figure 13 smaller temperature variation between top and bottom in the cladding of the central sphere CFC structure. The maximum temperature in the center of the sphere structures CS, CCC and CFC were equal to 1032° C, 1021° C and 1007° C, respectively. These temperatures are lower than the maximum specified operating temperature of the fuel in the PBMR design, which is equal to 1130° C (Lee et al. 2007a).

The pressure drop for the flow length (Pa/mm) with its respective maximum deviation of the time average of the structures CS, CCC and CFC was equal to 8.47 ± 0.11, 39.81 ± 0.29, 129, 22 ± 3.35, respectively.

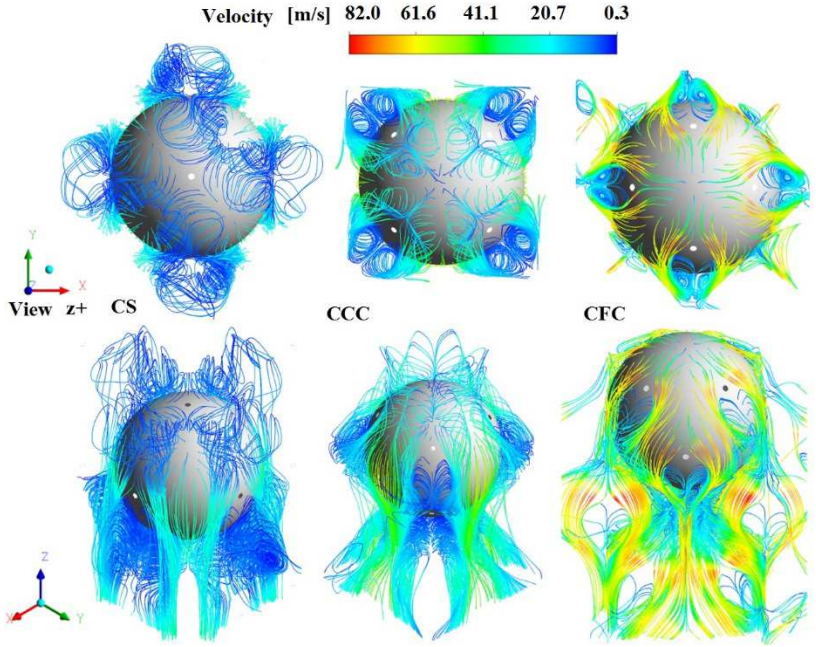

Figure 12.Streamlines around the center sphere.

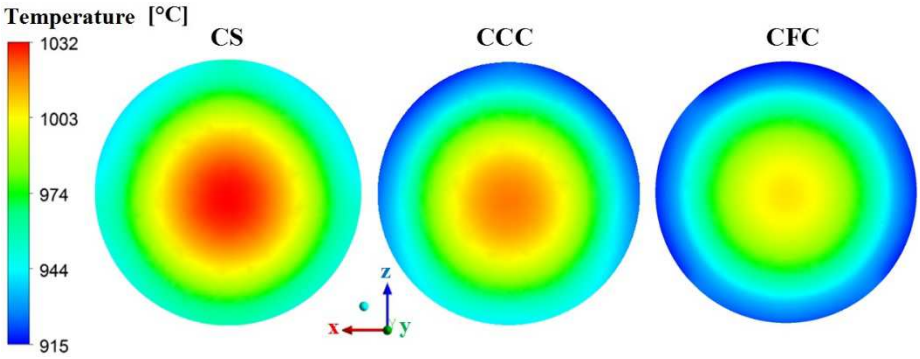

Figure 13.Temperature distribution within the central sphere.

Data from the pressure drop per length of flow (pressure differential / L) were compared with the Carmen-Kozeny equation. The Carmen-Kozeny equation with coefficient of friction as Van Der Walt (2006) and described by Equation 9 is a semi-empirical correlation obtained with measurements of pressure drop runoff and regular structures such as CS, CCC and CFC structures. The variables not defined in Eq. 9 is the fluid density (ρ), the flow velocity in the field without the ball (U) and the diameter of the spheres (d).

$$\frac{\Delta P}{L} = \frac{U^2 \rho FE}{d(1-FE)^3} X \frac{0{,}351}{Re/FE^{0{,}05} - 1{,}2} \qquad (9)$$

This Kozemy-Carmen equation is applicable for flows with *Re*/Fe from 2500 to 60000 in structures with packing factor of 0.118, and 0.65 (Van der Walt, 2006). Furthermore, Equation 9 disregards

the effects of flow input and output in packed bed. Table 6 shows the flow pressure drop per length calculated using Kozemy-Carmen equation and numerically for the three structures.

Table 6. Flow pressure drop.

	CS	CCC	CFC
Re/FE	52600	40250	37000
Semi-empirical. [Pa/mm]	8.56	39.50	81.31
Numerical [Pa/mm]	8.47	39.81	129.22
Difference [%]	-1.05	0.77	58.93

The *Re/FE* ratio of the three structures simulations is within the applicable range of Kozemy-Carmen equation, however, the packing factor structures CCC and CFC are outside this range. The numerical results of pressure drop were similar to those obtained with Equation Kozemy-Carmen (Van Der Walt, 2006) for CS and CCC structures. The packing factor of the CCC structure is somewhat removed from the valid range of the equation Kozemy-Carmen and probably for this reason the numeric value was close to the empirical. However, the numerical result of CFC structure showed a difference of 60% in relation to the semi-empirical results. This can be explained by the packing factor of this structure is considerably distant from the valid range of Equation 9 and the turbulence model used in the simulations.
Figure 14 shows the velocity of friction profile previously set, on the surface of the central sphere CFC structure of two analyzes.

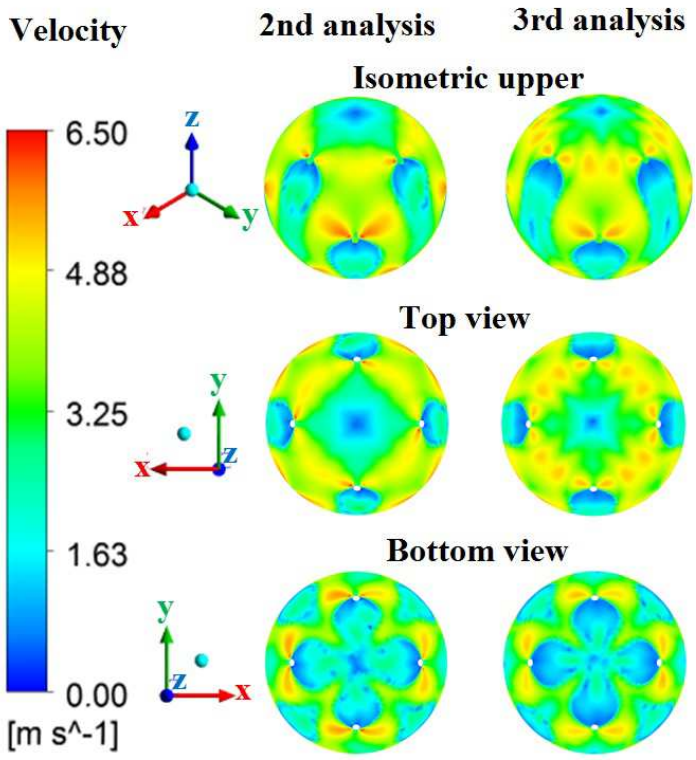

Figure 14.Friction velocity at the surface of the central sphere of the CFC model.

The temperature profile at the surface of the central sphere of the CFC model in both analyzes are compared in Figure 15 and graphically in Figure 16. The coordinates of the graph in Figure 16 are defined as in Figure 10. The average surface temperature of the sphere of the analysis was equal to 918.46 °C.

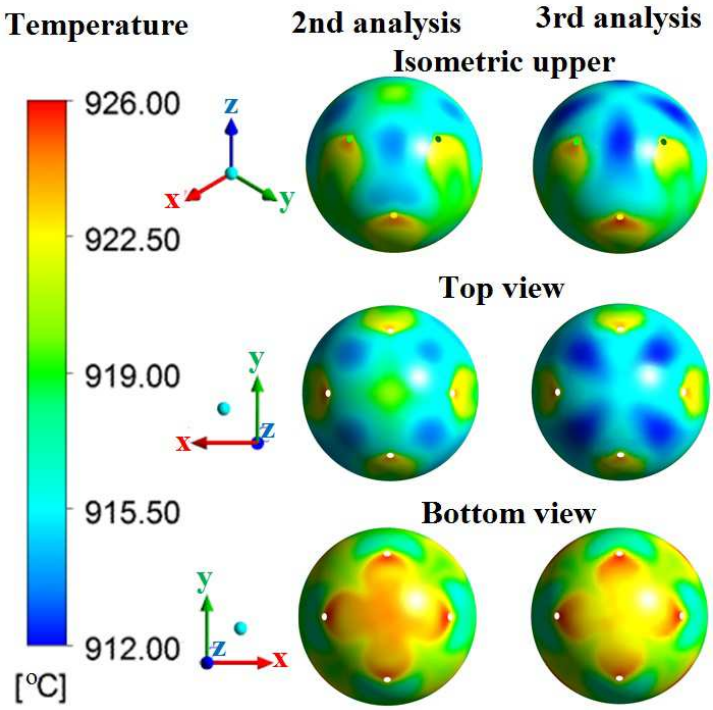

Figure 15.Temperature profile at the surface of the central sphere CFC model

The loss of charge by length and average *Nusselt* in the central sphere of the third CFC structure analysis were equal to 131.24 kPa/m 601.14 kPa/m, respectively. In the previous analysis of Santos et al. (2013) the pressure drop decreased by ~ 6% and the *Nusselt*increased ~ 25%

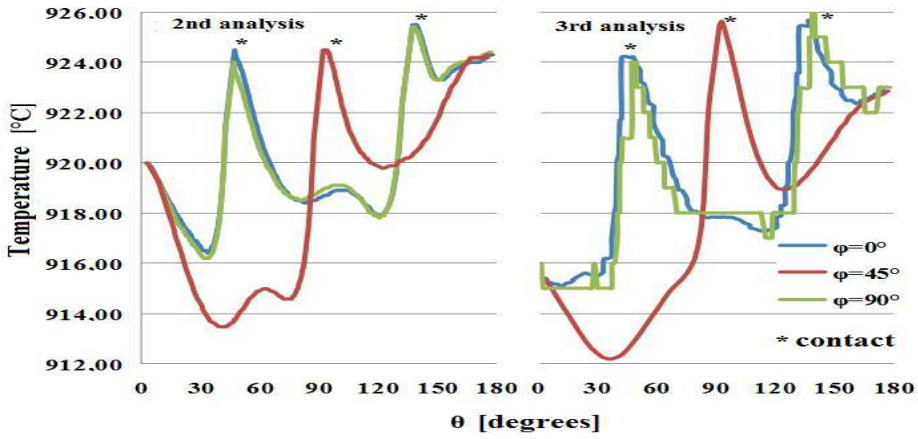

Figure 16.Temperature distribution on the surface of the central sphere of CFCs structure.

CONCLUSION

It was performed a numerical investigation of flow and heat transfer between coolant and fuel spheres present in the core of a PBR using the CFD code CFX 14.0 (Ansys, 2012). The study was done using three models, the first two being presented previously by Santos et. al (2013), and the third was presented here.

In this analysis, the spheres of structures CS and CCC show variations in surface temperature of approximately 30 °C. The surface temperature distribution in the sphere of CFC structure was more homogeneous with a maximum variation of 10 °C. Pressure loss per length of flow calculated numerically to CS and CCC structures varied at most 1% as compared using Kozemy-Carmen equation. However, the numerical result of CFC structure showed a difference of 60% in relation to the semi-empirical results. This can be explained by the packing factor of this structure is considerably distant from the valid range of Kozemy-Carmen equation and the turbulence *Standard k-ε* model.

The difference between the average *Nu* number using the correlation and *Nu* number obtained by CFC structure was equal to56%.It is believed that the turbulence model *Standard k-ε* used in the simulations could not calculate the flow in a manner acceptable in CFC structure resulting from this difference. The maximum temperature in the center of the sphere of the structures CS, CCC and CFC were equal to1032°C,1021°Cand 1007°C, respectively. These temperatures are lower than the maximum operating temperature of the fuel in the PBMR project, which is equal to1130°C.

The results presented are preliminary and needs to be other numerical and experimental results of investigations for its validation. It is suggested the creation of a model with random arrangement of spheres. The algorithms present in the work of Auwerda, GJ et al. (2010) can be used for this arrangement. The boundary condition at the input should be moved into a velocity profile that considers the flow between the upper spheres and the distribution of mass flow along the cross section of the core. It is suggested also conduct a study to estimate the numerical uncertainty due to mesh. The results obtained with other turbulence models should be evaluated in the simulations of flow in pebble bed. It is also suggested the application of the model *RANS k-ω* and *LES* method in such simulations, as proposed by Lee et al. (2007b).

ACKNOWLEDGEMENTS

The following Brazilian institutions support this research project: Nuclear Technology Development Centre (CDTN), Brazilian Nuclear Energy Commission (CNEN), Research Support Foundation of the State of Minas Gerais (FAPEMIG), Brazilian Council for Scientific and Technological Development (CNPq), and Brazilian Institute of Science and Technology (INCT).

REFERENCES

[1]. ACHENCACH, E. Heat and Flow Characteristics of Packed Beds.Experimental Thermal and Fluid Science, v.10, **1995**.

[2]. ANSYS Canada Ltd. CFX-14.0 Manuals, ANSYS Canada Ltd., Ontario, Canada, **2012**.

[3]. Auwerda, G.J., Kloosterman, J.L., Winkelman, A.J.M., Groen, J. and van Dijk, V., Comparison of Experiments and Calculation of Void Fraction Distributions in Randomly Stacked Pebble Beds, PHYSOR 2010 – Advances in Reactor Physics to Power the Nuclear Renaissance. **2010**.

[4]. Auwerda, G.J.; Kloosterman, J. L.; Winkelman, A. J.M.; Groen, J.; Dijk, V. van. Comparison of Experiments and Calculations of Void Fraction Distributions in Randomly Stacked Pebble Beds. PHYSOR 2010 - Advances in Reactor Physics to Power the Nuclear Renaissance, Pittsburgh, Pennsylvania, USA. **2010**.

[5]. Costa, F.C., Navarro, M.A., and Santos, A.A.C. Numerical Investigation of Flow in Bed Pebbles Gas Cooled High Temperature Reactors. In: International Nuclear Atlantic Conference - INAC. Belo Horizonte (in Portuguese). **2011**.

[6]. Dijk, V.V. Radial void fraction measurement of a randomly packed pebble-bed. Delft University of Technology, The Netherlands, **2008**.

[7]. Dijk, V.V. Radial void fraction measurement of a randomly packed pebble-bed. Delft University of Technology, The Netherlands, **2008**.

[8]. Duarte, J.P., Oliva, J.J.R. and Melo, P.F.F.F. Generation IV Nuclear Systems: State of the Art and Current Trends with Emphasis on Safety and Security Features. In: Current Research in Nuclear Reactor Technology in Brazil and Worldwide, Prof. Amir Mesquita (Ed.), InTech, Croatia. DOI: 10.5772/53140. **2013**.

[9]. Hassan, Y.A. Large eddy simulation in pebble bed gas cooled core reactors. Nuclear Engineering and Design, V. 238, I. 3, p. 530-537. March 2008. DOI: http://dx.doi.org/10.1016/j.nucengdes.**2007**.02.041.

[10]. Hore-Lacy, I., Nuclear Energy in the 21st Century. 2nd Edition, Word Nuclear University, London, 2011.

[11]. Lee, J.J., Park, G.C., Kim, K.Y., and Lee, W.J., Numerical treatment of pebble contact in the flow and heat transfer analysis of a pebble bed reactor core, Nuclear Engineering and Design, v. 237, p.2138-2196. **2007a**.

[12]. Lee, J.J., Yoon, S.J., Park, G.C., and Lee, W.J., Turbulence-Induced Heat Transfer in PBMR Core Using LES and RANS. Journal of Nuclear Science and Technology, v. 44, n. 7, p. 985-996, **2007b**.

[13]. Lohnert, G., Technical design features and essential safety-related properties of the HTR-module, Nuclear Engineering and Design. 121. **1990**.

[14]. Lohnert, G., and Reutler, H.The modular HTR-a new design of high temperature pebble bed reactor. J. Br. Nuclear Energy Soc. 22 June (3). 197. **1983**.

[15]. Matzner,H.D., PBMR project status and the way ahead. 2nd International Topical Meeting on High Temperature Reactor Technology, Beijing, China, September. **2004**.

[16]. Mclaughlin, B.; Worsley, M., Stainsby, R. Development of Local Heat Transfer and Pressure Drop Models for Pebble Bed High Temperature Gas-Cooled Reactor Cores.Proceedings of the 4th International Topical Meeting on High Temperature Reactor Tech, Washington, DC, USA. **2008**.

[17]. Mclaughlin, B.; Worsley, M., Stainsby, R. Development of Local Heat Transfer and Pressure Drop Models for Pebble Bed High Temperature Gas-Cooled Reactor Cores.Proceedings of the 4th International Topical Meeting on High Temperature Reactor Tech, Washington, DC, USA. **2008**.

[18]. NIST, Thermo physical properties of fluid systems, National Institute of Standards and Technology - NIST, http://webbook.nist.gov/chemistry/fluid/, **2013**.

[19]. Santos, A.A.C. Costa, F.C; Mesquita, A.Z.; Rezende, H.C. Numerical Investigation of Flow in Generation IV Pebble Bed Gas Cooled Core Reactors. International Journal of Energy and Power Engineering, v. 2, p. 69-76. DOI: 10.11648/j.ijepe.20130202.16. **2013**.

[20]. Sobes, V.; Forgetb, B., and Kadakc, A., "Individual pebble temperature peaking factor due to local pebble arrangement in a pebble bed reactor core".Nuclear Engineering and Design, v. 241, p. 124-133, **2011**.

[21]. Tak, N.I., Kim,Y.W., Choi, J.H., and Lee, W. J., Thermo-fluid investigation on a double- side-cooled annular fuel for the prismatic very high temperature gas-cooled reactor, Nuclear Engineering and Design, v. 238, p. 2821-2827, **2008**.

[22]. Van Der Walt, A.J.K. Pressure Drop through a Packed Bed. 2006. 116 f. Master's Dissertation - Post-graduate School of Nuclear Science and Engineering, North-West University, South Africa, **2006**.